Journal of Chemical Physics, 2008, vol. 129, no. 19, p. 194511.

Equilibrium fluctuations of the Lennard-Jones cluster surface

D. I. Zhukhovitskii*
Joint Institute of High Temperatures, Russian Academy of Sciences, Izhorskaya 13/19, 125412 Moscow, Russia
(Dated: November 28, 2008)

Spectra of the cluster surface equilibrium fluctuations are treated by decomposition into the bulk and net capillary ones. The bulk fluctuations without capillary ones are simulated by the surface of a cluster truncated by a sphere. The bulk fluctuations spectrum is shown to be generated primarily by the discontinuity in spatial distribution of cluster internal particles. The net capillary fluctuations slice spectrum is obtained in molecular dynamics simulation by subtraction of the bulk fluctuations spectrum from the total one. This net spectrum is in the best agreement with a theoretical estimation if we assume the intrinsic surface tension to be independent of the wave number. The wave number cutoff is brought in balance with the intrinsic surface tension and excess surface area induced by the capillary fluctuations. It is shown that the ratio of the ordinary surface tension to intrinsic one can be considered as a universal constant independent of the temperature and cluster size.

PACS numbers: 68.10.-m, 68.10.Cr, 68.10.Et

I. INTRODUCTION

The capillary wave model[1,2] (CWM) is now considered as a promising way of doing interface investigation, which can remove discrepancies between theory, experiment, and numerical simulation. Among widely discussed items are, e.g., the problem of interface thickness divergence and the form of density dependence on the coordinate normal to the interface. CWM considers an imaginary fluctuation surface assigned to any instant configuration of molecules at the interface. Fluctuations of this surface are treated in a macroscopic way using the classical capillary wave Hamiltonian. Unification of CWM, microscopic definition of the fluctuation surface, and density functional theory is now in progress.[3,4] In recent studies, attention was focused on the microscopic structure of the interfaces between liquid and vapor or two immiscible liquids. Such studies assume numerical simulation by Monte Carlo[5] and molecular dynamics (MD) methods.[6,7] Microscopically defined fluctuation surface was treated by Tarazona and Chacón[5] and Chacón *et al.*[8] for the liquid–vapor interface, and by Chowdhary and Ladanyi,[6,7] for the liquid–liquid interface. These simulations revealed strong oscillations of the density defined relative to the fluctuation surface. The same effect for water was displayed in Ref.[8]. The wave number spectrum of capillary fluctuations showed relatively fast decay, and the effective intrinsic surface tension seemed to increase substantially with the wave number.[5] Models for the interacting surfaces of immiscible liquids and their wave number spectra led to the conclusion about the importance of both the bulk fluctuations, which dominate in the short-wavelength spectral region, and a correct wave number cutoff criterion.[7] The importance of a correct identification of capillary and bulk fluctuations was discussed by Stillinger,[9] who proposed to introduce a subset of inherent structures and to define an intrinsic density profile free of the capillary fluctuations.

Study of clusters is an independent field of research, which can represent a complementary method for the investigation of liquid–vapor interface. The surface of a sufficiently large cluster is a good approximation to the flat interface; at the same time, variation of cluster radius allows investigation of the curvature effect. The wave number and frequency Fourier spectra were calculated in MD simulation of the Lennard-Jones clusters in Ref.[10], where the surface particles that mark the fluctuation surface were defined as the most external cluster particles, which form percolating umbrellas over the internal particles.[11] The main conclusion of this study, which we will refer to as the previous study, is a considerable discrepancy between the calculated spectrum and predictions of the early version of CWM applied to liquid clusters[12] both in the wave number and temperature spectral dependences. However, theoretical analysis in the previous study was restricted to an order of magnitude estimate of the spectral density. To our knowledge, no analysis of the liquid cluster surface fluctuations was undertaken in the literature.

The objective of this paper is to give a detailed analysis and theoretical interpretation of the results obtained in the previous study. The spectral densities calculated in this MD simulation are treated as a sum of two components, the net capillary and bulk fluctuations. The latter are estimated using the procedure for a free cluster surface applied for the clusters truncated by a sphere, which removes the surface and some adjacent particles. Truncation is assumed to prepare a particle configuration with the surface particles most closely approaching an ideal sphere undisturbed by the capillary fluctuations. Thus, we can associate such configuration with the absence of capillary fluctuations and calculate the bulk fluctuations wave number spectrum. This spectrum estimated using MD data can be reproduced to a good accuracy in a simple model assuming random uniform spatial distribution of the internal (bulk) particles. Therefore, discontinuity of cluster bulk rather than instantaneous density nonuniformity proves to be a reason for the bulk fluctuations. Net capillary fluctuations spectrum is then obtained as a difference between the total and bulk spectrum. The net

spectrum associated with CWM is restricted by a short-wavelength cutoff that confines the curvature of capillary fluctuation surface. Such cutoff turns out to be of the order of several interparticle distances and is therefore larger than the cutoff of common occurrence.

To compare the CWM with modified cutoff and MD simulation results directly, a recalculation of theoretical 2D spherical spectra to one-dimensional slice spectra was performed. Here, net slice spectra were calculated for individual spherical harmonics. The sum of all spectral amplitudes was found to be in a reasonable agreement with net slice spectra obtained in MD simulation, which corroborates a theoretical approach developed in this paper.

The paper is organized as follows. In Sec. II, the bulk fluctuations are defined and determined from MD data and theoretical considerations, in Sec. III, the intrinsic surface tension and short-wavelength cutoff dependent on the excess surface area are discussed, and in Sec. IV, theoretical estimates for one-dimensional slice spectra are obtained and compared with the spectra calculated using MD simulation. The results are summarized in Sec. V.

II. BULK FLUCTUATIONS

In this Section, a method of capillary and bulk fluctuations decomposition is developed. The system under consideration consists of an isolated cluster in the state of unstable equilibrium with surrounding vapor of monomers (clusters in the vapor are ignored). The system is characterized by the constant temperature T and vapor number density n_v. Such system was simulated in the previous study using the (P, T)-ensemble method, in which the cluster under investigation is situated close to the center of a spherical cell; the cell surface performs the function of vapor particles generation and removal. The Lennard-Jones interaction potential between two particles has the form

$$u(r) = \begin{cases} v(r) - v(r_c), & r \le r_c, \\ 0, & r > r_c, \end{cases} \qquad v(r) = 4\varepsilon \left(\frac{a^{12}}{r^{12}} - \frac{a^6}{r^6} \right), \tag{1}$$

where r is the interparticle distance; $r_c = 2.5a$ is the cutoff radius; ε is the well depth; and a is the length scale. In this paper, we use the MD units: $\tau_0 = a\sqrt{M/24\varepsilon}$ for the time (M is the particle mass); a for the distance; a^{-3} for the particle density; ε for the energy and temperature, and ε/a^2 for the surface tension.

Calculation of the wave number spectra was performed in the previous study for the surface particles confined within two parallel planes at the distance $h/2 = 1/2\sqrt{3}n_\ell^{1/3}$ from cluster center of mass each. Here, n_ℓ is the number density of internal cluster particles, i.e., the bulk number density. We will call such one-dimensional spectra the slice spectra. The definition of surface particles is given by Eq. (2) of Ref.[10]. It is based on widely discussed assumption concerning the spatial homogeneity of a cluster (or liquid slab in the simulation with a flat interface) and abrupt drop of particle number density at cluster surface (see Refs.[10,11] and references therein). This implies existence of a single monolayer of the surface particles that have a reduced number of nearest neighbors as compared to the internal particles. The above-mentioned definition of these particle types postulates that for each internal particle of a sufficiently large cluster, there exists at least one outermost surface particle, whose "umbrella" of the radius h covers this particle. Note that such definition of the outermost layer of particles and resulting identification of the fluctuation surface is qualitatively similar to that proposed by Stillinger.[13] The value $h = 1/\sqrt{3}n_\ell^{1/3}$ was selected to ensure the best fit of surface and internal particle distributions over the number of bonds to respective Gaussian exponents in the expansion of total distribution in the pair of exponents. In the slice snapshots like Fig. 1 in Ref.[10], the surface particles really seem to form a monolayer over the internal particles. One can verify that small variations of h would not change this situation. However, a substantial change leads to obvious surface layer distortions. Thus, the decrease in h depletes the monolayer (internal particles take the place of surface ones); the increase of h results in the intrusions of surface particles in the bulk of a cluster. In both cases, the distributions over number of bonds for both particle types deviate from the Gaussian type. Therefore, an appropriate choice of the surface particles allows using them as pivots for the fluctuation surface and its cross sections analyzed in the previous study.

To decompose the surface and bulk fluctuations, we will focus our attention on the latter and formulate the procedure that makes it possible to estimate the bulk fluctuation spectrum. At the first step, we will define a configuration with zero capillary fluctuation. It is natural to assume that for such configuration, any thermodynamic potential quantity (in treated case, the Gibbs free energy) includes no term corresponding to the fluctuations other than the ones that occur in the bulk. Therefore, we must construct such configuration solely of internal particles. If all surface particles would lie on a spherical surface, the capillary fluctuations were equal to zero identically. However, the probability to find such configuration is equal to zero. It is then necessary to select a set of configurations in the vicinity of such improbable one (this conforms to the idea of Ref.[9]). To make this selection usable for numerical simulation, we define a configuration with no capillary fluctuation as the cluster truncated by a sphere with the radius $\bar{R}$ smaller than the minimum distance between a surface particle and the cluster center of mass. In other words, all the surface and some internal particles at the distances larger than $\bar{R}$ are removed.

The slice spectra were calculated for truncated clusters

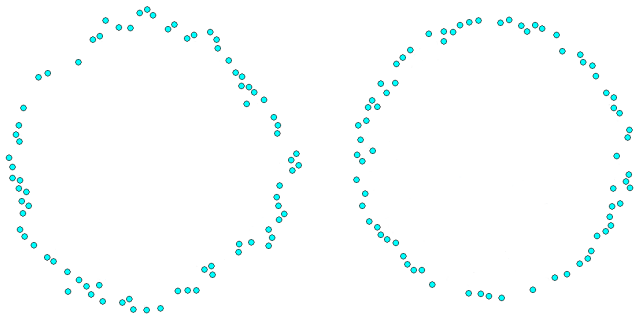

FIG. 1: The slice snapshots of surface particles for the free surface (left) and truncated cluster (right) at $g = 20000$ and $T = 0.75$.

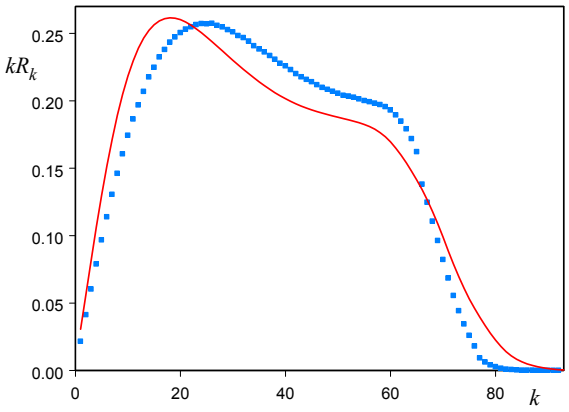

FIG. 2: Bulk fluctuations spectra scaled to the cluster size $g = 30000$ at $T = 0.75$ calculated from MD simulation data (truncated clusters, dots) and by Eqs. (2) and (3) (line).

following the method discussed in detail in the previous study. We used also the cluster configurations obtained therein, which have been stored for the runs at $T = 0.75$ and the clusters including initially $g = 30000$ particles. Truncation at $\bar{R} = 18.4$ guaranteed that only the internal particles were retained; the cluster size was decreased down to 20000. Then, the surface particles were identified and isolated for *truncated* clusters in the same way it was done for the free surface (for truncated clusters, the result is naturally insensitive to the removal of virtual chains). A slice was formed by the particles falling between two planes at the distance $h = 0.6$, with the cluster center of mass at the half-distance. Figure 1 presents snapshots of the surface particles for the free surface and the surface of a truncated cluster. Long-wavelength fluctuations are recognizable on the free surface, and the amplitude of bulk fluctuations with predominantly short wavelengths on the truncated surface is noticeably high.

The slice surface particles with polar coordinates (r_i, φ_i) were considered as pivots for a continuous periodical function $\tilde{P}(\varphi)$, whose values are known at random points, $\tilde{P}(\varphi_i) = r_i$. $\tilde{P}(\varphi)$ was resampled to the analytical grid and then Fourier analyzed for different slices corresponding to cluster rotation relative to the slice plane. Its squared spectral amplitude was averaged over the rotation angles and cluster configurations to calculate the spectrum of bulk fluctuations R_k as a function of the mode number k. Note that for R_k, the convergence of averaging is much faster than that for the free surface. Variation in $\bar{R}$ in relatively wide limits reveals scaling property of kR_k, which is much more accurate than for the total spectrum (see Fig. 4b of Ref.[10]). Given the temperature, kR_k is a universal function of $k/\bar{g}_{cs}$, where $\bar{g}_{cs}$ is the average number of surface particles in a slice. After scaling, respective dots almost coincide. The bulk fluctuation spectrum scaled to the initial cluster size is shown in Fig. 2. At small k, R_k varies slowly; at large k, R_k vanishes due to finiteness of $\bar{g}_{cs}$.

It will be shown below that R_k can be calculated within a simple model. We will assume a random uniform spatial distribution for all cluster particles and ignore correlations of their positions. Then φ is uniformly distributed on the interval $0 \le \varphi < 2\pi$, and the value of function $\tilde{P}(\varphi)$, on $\bar{R} - \Delta < \tilde{P}(\varphi) < \bar{R}$, where Δ is the distribution width. Hence, the probability to find a particle at the distance between r and $r + dr$ from the origin of the coordinate system, which is assumed to coincide with the cluster center of mass, is

$$p_r(r)\,dr = \begin{cases} dr/\Delta, & \bar{R} - \Delta < r < \bar{R}, \\ 0, & r \le \bar{R} - \Delta \text{ or } r \ge \bar{R}, \end{cases} \qquad (2)$$

and the distribution for φ has similar form. The probability to find a surface particle in a given slice is $p_{cs} \simeq h/2\bar{R} \ll 1$. If g_s is the total number of surface particles, $\bar{g}_{cs} = p_{cs} g_s$ coincides with the variance of the number of surface particles in a slice g_{cs}. Hence, the probability distribution to find g_{cs} surface particles in a slice has the Gauss form

$$p_g(g_{cs}) = \frac{1}{\sqrt{2\pi\bar{g}_{cs}}} \exp\left[-\frac{(g_{cs} - \bar{g}_{cs})^2}{2\bar{g}_{cs}}\right]. \qquad (3)$$

An independent numerical simulation of the bulk fluctuations was performed as follows. First, the number g_{cs} was generated at random with probability distribution (3), where $\bar{g}_{cs} = 76$ was calculated from MD data. Then g_{cs} pairs of polar coordinates were generated with distribution (2). The function $\tilde{P}(\varphi)$ obtained in such a way was resampled to an analytical grid and Fourier analyzed. Averaging over 10^6 realizations of this procedure yields a model bulk fluctuations spectrum shown in Fig. 2. In this simulation, Δ was adjusted to fit the distribution obtained from the MD data; the best fit value proved to be of the order of the distance between surface particles, $\Delta \simeq 2\pi\bar{R}/\bar{g}_{cs}$. A good correlation between independent estimations of R_k seen in Fig. 2 is evidence of the fact that the basic reason of the bulk fluctuations treated in this paper is the discontinuity of cluster bulk.

For a crude estimation of R_k, we can assume that $\tilde{P}(\varphi)$ has the uniform distribution, and distribution (3) has a zero width, i.e., $g_{cs} \equiv \bar{g}_{cs}$. Then the bulk fluctuations

are white noise, and R_k is constant in the interval of mode numbers from 1 to $\bar{g}_{cs}$, which in this simplified case is the highest mode number. The contribution of bulk fluctuations to the total fluctuation variance defining the interface width is then

$$\sigma_b^2 = \frac{1}{2}\sum_{k=1}^{\bar{g}_{cs}} R_k = \frac{\bar{g}_{cs}R_1}{2} = \frac{\Delta^2}{12}. \tag{4}$$

Estimation (4) is indicative of the fact that σ_b^2 *does not diverge* both at small and large g. The scaling law is obvious from Eq. (4):

$$kR_k = kR_1 = \frac{k\Delta^2}{6\bar{g}_{cs}}, \tag{5}$$

i.e., kR_k depends solely on $k/\bar{g}_{cs}$. Since $\bar{g}_{cs} \propto \bar{R}$, kR_k is also scaled with $k/\bar{R}$.

As is seen in Fig. 2, the bulk fluctuations spectrum deviates from the white noise one. This is caused by converting the random values of φ to analytical grid. To conserve the variance of original pivots, their number must be less than that of points on the analytical grid (see the discussion in Sec. IV), whence it follows that some values of $\tilde{P}(\varphi)$ at neighboring grid points are equal. This implies a buildup of R_k for small k. If we did not ignore particle correlations, less number of $\tilde{P}(\varphi)$ values would coincide, and R_k would be less different from white noise in the long-wavelength region. This clarifies the less pronounced buildup in this region for R_k calculated from MD data.

In spite of the deviation of MD R_k from the white noise distribution, its variance can be to high precision approximated as follows [see Eq. (4)]:

$$\sigma_b^2 = \sum_{k=1}^{k_{\max}} R_k \simeq \frac{\Delta^2}{12} + \delta g^{-1/3}, \tag{6}$$

where for $T = 0.75$, $\Delta = 2.0$ and $\delta = -0.8$; summation extends up to $k = k_{\max}$, at which R_k vanishes; this approximation is valid at $g > 400$. Equation (6) defines the contribution from bulk fluctuations to the total interface variance. As regards the spectral density of net capillary fluctuations Q_k, one can write it in the form

$$Q_k = S_k - R_k, \tag{7}$$

where S_k is the total spectral density.

III. CAPILLARY FLUCTUATIONS

Consider the CWM for an isotropic cluster. We will use the formalism proposed first by Rayleigh[14] for treatment of liquid drop oscillations. Since any real configuration includes the bulk fluctuations, a net capillary fluctuation does not exist, and, therefore, it is impossible to formulate an appropriate microscopic definition. We will treat the fluctuations not included in the set of bulk ones, which give rise to some *mesoscopic* excess surface area, and call them the capillary fluctuations. According to CWM we write the additional Gibbs free energy of their formation in the form

$$\Phi = \gamma_0 \Delta A = \frac{\gamma_0}{2}\int\limits_{\Omega} |\nabla\xi(\mathbf{r})|^2\, dS, \tag{8}$$

where γ_0 is the intrinsic surface tension; ΔA is the excess surface area induced by a fluctuation; integral (8) is taken over the entire cluster equimolar surface Ω with the radius R, and $\xi(\mathbf{r})$ is the position of fluctuation surface relative to Ω, so that $\int\limits_{\Omega} dS = 4\pi R^2$, $\int\limits_{\Omega} \xi(\mathbf{r})\, dS = 0$. It is assumed that in the spherical coordinates $(r,\, \vartheta,\, \varphi)$, the fluctuation surface is defined by the equation $r = R + \xi(\vartheta,\, \varphi)$. Note that Eq. (8) implies that γ_0 is independent of the wave vector (see Sec. IV) and the fluctuation amplitude is small so that $|\nabla\xi(\vartheta,\, \varphi)| \ll 1$. In contrast to the previous study, we use γ_0 instead of the ordinary surface tension γ.

We expand $\xi(\vartheta,\, \varphi)$ in spherical harmonics $Y_{lm}(\vartheta,\, \varphi)$,

$$\xi(\vartheta,\, \varphi) = R\sum_{l,m} a_{lm} Y_{lm}(\vartheta,\, \varphi), \tag{9}$$

where $-l \le m \le l$, to derive

$$\begin{aligned}\Phi &= \frac{\gamma_0 R^2}{2}\int\limits_{\Omega} |\nabla\xi(\vartheta,\, \varphi)|^2 \sin\vartheta\, d\vartheta d\varphi \\ &= \frac{\gamma_0 R^2}{2}\sum_{l,m} |a_{lm}|^2 (l-1)(l+2).\end{aligned} \tag{10}$$

Note that if $|a_{lm}| \ll 1$, expansion (9) conserves the cluster volume, $\int\limits_{V} d^3\mathbf{r} = (4\pi/3)R^3$, where V is the volume bounded by the fluctuation surface $r = r(\vartheta,\, \varphi)$; the momentum conservation dictates that $l \ge 2$.

The expression for average squared expansion amplitude follows from the equipartition theorem:

$$\left\langle |a_{lm}|^2 \right\rangle = \frac{T}{\gamma_0 R^2 (l-1)(l+2)}. \tag{11}$$

This means that $\left\langle |a_{lm}|^2 \right\rangle$ is independent of m, and Eq. (11) is actually the approximation of linear independent modes. The latter is a consequence of the assumptions that $|a_{lm}| \ll 1$ and γ_0 is independent of l, m.

We average Eq. (10) to deduce the excess surface area

$$\langle \Delta A \rangle = \frac{\langle \Phi \rangle}{\gamma_0} = \frac{R^2}{2}\sum_{l,m} \left\langle |a_{lm}|^2 \right\rangle (l-1)(l+2). \tag{12}$$

Substitution of Eq. (11) into Eq. (12) yields $\langle \Delta A \rangle = (T/2\gamma_0)\sum\limits_{l} (2l+1)$, which diverges at large l. We introduce the largest (cutoff) number $l = \Lambda$ to make $\langle \Delta A \rangle$

finite:

$$\langle \Delta A \rangle = \frac{T}{2\gamma_0} \sum_{l=2}^{\Lambda} (2l+1) \simeq \frac{T\Lambda^2}{2\gamma_0}, \tag{13}$$

if $\Lambda \gg 1$. Since the cluster is isotropic, averaging Eq. (8) yields one more relation for $\langle \Delta A \rangle$:

$$\langle \Delta A \rangle = \frac{1}{2} \int_{\Omega} \left\langle |\nabla \xi(\vartheta, \varphi)|^2 \right\rangle dS = 2\pi R^2 \kappa^2, \tag{14}$$

where $\kappa = \sqrt{\left\langle |\nabla \xi(\vartheta, \varphi)|^2 \right\rangle}$ is the root-mean-square gradient of the capillary fluctuation surface. According to the previous study if we exclude virtual chains of particles (overhangs), for which $|\nabla \xi(\vartheta, \varphi)| \gtrsim 1$, the remaining surface satisfies the condition $|\nabla \xi(\vartheta, \varphi)| \lesssim 1$. Hence, one could expect that κ was some constant of the order of unity and that the ratio $\langle \Delta A \rangle / 4\pi R^2 = \kappa^2/2$ was independent of the temperature and cluster size. We compare Eqs. (13) and (14) to deduce the cutoff number

$$\Lambda = 2R\kappa \sqrt{\frac{\pi \gamma_0}{T}}. \tag{15}$$

It follows from the definition of the ordinary surface tension γ, $4\pi R^2 \gamma = 4\pi R^2 \gamma_0 + \langle \Delta A \rangle \gamma_0$, and Eq. (14) that γ_0 is related to γ as

$$\frac{\gamma}{\gamma_0} = 1 + \frac{\kappa^2}{2}. \tag{16}$$

Thus, the ratio γ/γ_0 is a constant greater than unity ($\kappa^2 > 0$). We substitute γ_0 from Eq. (16) into Eq. (15) to eventually derive

$$\Lambda(\kappa) = R\kappa \left[\frac{8\pi\gamma}{(2+\kappa^2)T} \right]^{1/2}. \tag{17}$$

The maximum wave number corresponding to cutoff (17)

$$q_{\max} = \frac{\Lambda}{R} = \kappa \left[\frac{8\pi\gamma}{(2+\kappa^2)T} \right]^{1/2} \tag{18}$$

is for treated conditions several times smaller than that corresponding to the interparticle distance.

The contribution from the capillary fluctuations to the total interface variance is [see Ref.[12] and Eq. (31)]

$$\begin{aligned} \sigma_c^2 &= \frac{R^2}{4\pi} \sum_{l=2}^{\Lambda} (2l+1) \left\langle |a_{lm}|^2 \right\rangle \\ &\simeq \frac{(2+\kappa^2)T}{8\pi\gamma} \ln \frac{(2\Lambda - 1)(2\Lambda + 5)}{7}. \end{aligned} \tag{19}$$

Since $\Lambda \propto R \propto g^{1/3}$, σ_c^2 [Eq. (19)] *diverges* as $\ln g$, which is similar to the variance divergence of a flat interface in the absence of gravity as the surface area is increased.[2]

IV. CWM SLICE SPECTRA

An objective of this Section is to calculate the slice spectra of net capillary fluctuations Q_k given its 2D spectrum [Eqs. (11) and (17)] and to compare the result with the slice spectra obtained in MD simulation. A single adjustable parameter in this calculation will be κ. The simplest way to do this is to create configurations with the net capillary fluctuations in the form of individual spherical harmonics. As in the foregoing, fluctuation modes are assumed to be independent. Therefore, each spherical harmonic with the numbers l, m must contribute additively to the squared spectral amplitude of the slice mode with the number k and can be treated separately.

We take an arbitrary configuration of particles stored during MD simulation corresponding to desired cluster size and isolate the surface particles. Within the accuracy of our calculations, the result proved to be fully insensitive to the choice of a concrete configuration because for each surface particle with the spherical coordinates $(r_i, \vartheta_i, \varphi_i)$, we substitute r_i for the coordinate of a capillary fluctuation in a special form. We use the relation $Y_{lm}(\vartheta, \varphi) \propto P_l^m(\cos\vartheta)\, e^{im\varphi}$, where $P_l^m(\cos\vartheta)$ is the Legendre function, to pass from the complex Fourier series (9) to real one and to write the new coordinate r_i as

$$r_i = R + A_{lm} \sqrt{\frac{T}{\gamma(l-1)(l+2)}}\, P_l^m(\cos\vartheta_i)\, \cos m\varphi_i. \tag{20}$$

Here, the normalization constant is

$$A_{lm} = \begin{cases} \left\{ 2\pi \int\limits_0^{\pi} [P_l^m(\cos\vartheta)]^2 \sin\vartheta\, d\vartheta \right\}^{-1/2}, & m = 0, \\ \left\{ \dfrac{\pi}{2} \int\limits_0^{\pi} [P_l^m(\cos\vartheta)]^2 \sin\vartheta\, d\vartheta \right\}^{-1/2}, & m > 0, \end{cases} \tag{21}$$

and we use the exact expressions for $P_l^m(\cos\vartheta)$ at $l \leq 5$ or $l = m$ [$P_l^l(\cos\vartheta) \propto \sin^l\vartheta$], and the asymptotic representation

$$\begin{aligned} &P_l^m(\cos\vartheta) \\ &\simeq \sin^{-1/2}(\vartheta) \cos\left[\left(l + \frac{1}{2} \right) \vartheta - \frac{\pi}{4} + \frac{\pi m}{2} \right], \end{aligned} \tag{22}$$

for $l > 5$ and $l \neq m$. Note that mode (20) corresponds to the average squared amplitude $\left\langle |a_{lm}|^2 \right\rangle = T/\gamma R^2 (l-1)(l+2)$, which includes γ rather than γ_0 [see Eq. (11)] because the latter depends on yet unknown κ. However, the problem linearity allows to correct this factor later.

For each surface particle configuration formed in such a way, we perform the slice Fourier analysis; i.e., we define a periodic function $\tilde{P}^{(l,m)}(\varphi_i) = r_i$ and expand it in the Fourier series (for a detailed discussion, see the previous

study)

$$\tilde{P}^{(l,m)}(\varphi) = \frac{\alpha_0^{(l,m)}}{2} + \sum_{k=1}^{k_{\max}} \alpha_k^{(l,m)} \cos k\varphi + \sum_{k=1}^{k_{\max}} \beta_k^{(l,m)} \sin k\varphi, \tag{23}$$

where $k_{\max}$ is the maximum mode number, at which Q_k is assumed to vanish. Then the cluster is rotated around the Euler angles ψ_1 and ψ_2, and the contribution from all l th spherical harmonics corresponding to the case $\gamma_0 = \gamma$ to the slice spectrum mode with the number k is calculated by averaging over slice amplitudes and summing over m:

$$\tilde{S}_k(l) = \sum_{m=0}^{l} \frac{\left\langle g_{cs} \left[\left(\alpha_k^{(l,m)}\right)^2 + \left(\beta_k^{(l,m)}\right)^2 \right] \right\rangle_{\psi_1,\psi_2}}{\langle g_{cs} \rangle_{\psi_1,\psi_2}}. \tag{24}$$

The rotation starts from random values of ψ_1 and ψ_2 generated for each spherical harmonic to eliminate the interference with zeros of spherical harmonics (result was found to be insensitive to these values). Hence, in the approximation of modes linearity and independence, we arrive at the capillary fluctuations slice spectrum

$$Q_k = \left(1 + \frac{\kappa^2}{2}\right) \sum_{l=2}^{\Lambda(\kappa)} \tilde{S}_k(l), \tag{25}$$

where the factor in parenthesis corrects the replacement of γ_0 by γ in Eq. (11), and the cutoff number $\Lambda(\kappa)$ is defined by Eq. (17).

We adjusted κ to fit Q_k [Eq. (25)] to the net spectrum of capillary fluctuations obtained in MD simulation. Calculations were performed for two temperatures (Fig. 3) at $\kappa = 0.548$, which provided the best fit. The slice widths $h = 0.60$ and 0.59 corresponded to the bulk liquid number densities $n_\ell = 0.76$ and 0.80 at $T = 0.75$ and 0.69, respectively. Figure 3 shows a fast decay of Q_k as k is increased. The spectral density of bulk fluctuations exceeds Q_k at $k > k_0$, where the threshold value k_0 is noticeably smaller than $k_{\max}$. It is noteworthy that for both temperatures at $k < k_0$, Q_k [Eq. (25)] was found to be almost independent of the slice thickness as it was varied within 15

One can estimate Q_k roughly assuming that the contribution from spherical harmonics with certain l is evenly distributed between slice modes with $k \le l$ (then the cutoff for k is Λ, same as for l). In addition, the harmonics with even l contribute solely to $l/2$ even slice modes (even k), and the harmonics with odd l contribute to $l/2$ odd slice modes (odd k). If a fluctuation was formed by the harmonics with a certain $l \gg 1$, the surface variance would be

$$\frac{l}{2}\frac{\tilde{S}_k(l)}{2} = \frac{R^2}{4\pi} \sum_{m=-l}^{l} \frac{T}{\gamma R^2 (l-1)(l+2)} \simeq \frac{T}{2\pi\gamma l}. \tag{26}$$

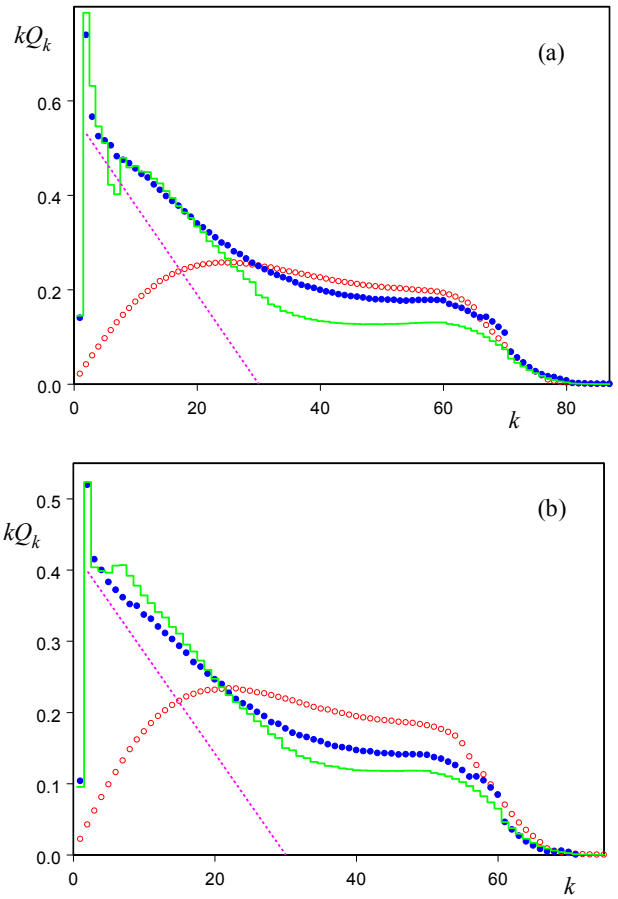

FIG. 3: Net slice spectra of the cluster capillary fluctuations for (a) $g = 30000$ and $T = 0.75$ and (b) $g = 19300$ and $T = 0.69$. Calculation by Eqs. (25) and (17) (solid line), rough estimation of Eq. (27) (dashed line), and estimation from MD simulation data (solid circles). The bulk fluctuation spectra (open circles) are shown for reference.

Then it follows from Eqs. (25) and (26) that

$$Q_k \simeq \left(1 + \frac{\kappa^2}{2}\right) \frac{2T}{\pi\gamma} \frac{1}{2} \sum_{l=k}^{\Lambda} \frac{1}{l^2} \simeq \left(1 + \frac{\kappa^2}{2}\right) \frac{T}{\pi\gamma} \left(\frac{1}{k} - \frac{1}{\Lambda}\right), \tag{27}$$

where the factor $1/2$ accounts for the summation over even or odd l. As is seen in Fig. 3, estimation (27) is in reasonable agreement with the numerical calculation of Q_k [Eq. (25)] at $k < \Lambda$. Vanishing of Eq. (27) at $k = \Lambda$ arises from the neglect of the spherical harmonics contribution to the slice modes with $k > l$. This contribution is unavoidable under the conditions that the ratio of spectral amplitudes at $l \sim 1$ and the maximum l is about 10^3. The low tail of capillary fluctuations spectrum at $k > \Lambda$ indicates the level of accuracy of the calculations including resampling procedure and numerical Fourier analysis rather than any physical reality: though cutoff (17) excludes capillary fluctuations at $l > \Lambda$, it is hard to elim-

inate the effect of harmonics with $l < \Lambda$ on the modes with $k > \Lambda$ in slice spectra.

The scaling law follows from Eq. (27):

$$kQ_k = \frac{T}{\pi\gamma_0}\left(1 - C\frac{k}{\bar{g}_{cs}}\right), \qquad (28)$$

where $C = \bar{g}_{cs}/\Lambda = (\Gamma h/4r_\ell^2\kappa)(T/\pi\gamma_0)^{1/2}$, $\Gamma = g_s g^{-2/3} \approx$ const, and $r_\ell = (3/4\pi n_\ell)^{1/3}$. At fixed temperature, kQ_k is a function of a single quantity $k/\bar{g}_{cs}$. It follows from scaling law (5) and relation (7) that the total slice spectral density $kS_k = kQ_k + kR_k$ is also scaled, as revealed in the previous study. For $1 \ll k \ll \Lambda$, $kQ_k \simeq T/\pi\gamma_0$, which, accurate to the substitution of γ_0 for γ, coincides with the spectral density of capillary fluctuations of a flat liquid interface at zero gravity.[2] Hence, in this limit, the difference between the cluster surface and a flat interface vanishes.

One can estimate the boundary $k = k_0$ between the small wave number region of capillary fluctuations and the large wave number region of bulk fluctuations by the relation $Q_{k_0} = R_{k_0}$. We derive the following from Eqs. (5) and (27)

$$k_0 = \left(\frac{\pi\gamma_0\Delta^2}{6\bar{g}_{cs}T} + \frac{1}{\Lambda}\right)^{-1}. \qquad (29)$$

For Figs. 3(a) and 3(b) $\bar{g}_{cs} = 76$ and 66, respectively, and $\bar{g}_{cs} = \Gamma h g^{1/3}/2r_\ell \propto g^{1/3}$ if $h \propto r_\ell$; corresponding k_0 [Eq. (29)] are equal to 21 and 19. This agrees with the results of numerical calculations of Q_k and R_k: $k_0 =$ 25 and 21, respectively (Fig. 3). It is worth mentioning that, unlike Λ [Eq. (17)], k_0 increases with the increase in temperature. However, these quantities are still not much different, $\Lambda = 29$ for both temperatures.

Since the cluster relaxation time is defined by the harmonics with $l = 2$ and it is relatively long, corresponding slice spectral densities S_k may be in error for the smallest k. To inspect this possibility, MD simulation of cluster evolution was performed once more for the same $T = 0.75$ and initial cluster size $g = 30000$ as in the previous study but for the vapor number density $n_v = 0.01402$, which was adjusted so that the cluster was very close to equilibrium (simulation cell radius was increased up to 42). Consequently, the cluster size did not change noticeably, and a single run was recorded in this simulation with the total time of cluster evolution of 36000 that was considerably longer than in the previous simulation ($\sim$ 7000). Cluster configurations from run start to the time of 8500 were ignored as nonequilibrium ones. It was found that during the averaging procedure, S_2 converged to the value of 0.7804 at $h = 0.6$, so that previous simulation underestimated this quantity by nearly 10 percent. A new run was performed for the lower temperature $T = 0.69$. For the cluster sizes, which varied from $g = 20000$ to 18700 during cluster evolution, this temperature was somewhat higher than the melting one. At this temperature and cluster size, the cluster is close to equilibrium with surrounding vapor if $n_v = 0.00771$.

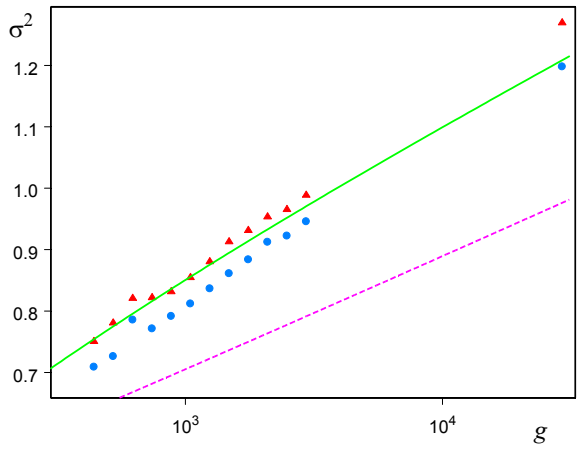

FIG. 4: Surface variance as a function of cluster size: direct calculation of the surface particles radial variance (triangles), estimation by the slice spectral amplitudes (circles); theoretical estimations with [solid line, Eqs. (6) and (19)] and without the account of bulk fluctuations and intrinsic surface tension [dashed line, Eq. (31)].

After the equilibration time of 10000, cluster configurations during the evolution time of 17500 were used to estimate the quantities S_k, R_k, and Q_k with $h = 0.59$. For both temperatures, when the slice thickness was varied, S_k and R_k changed but their difference Q_k was almost independent of the thickness.

Figures 3(a) and 3(b) demonstrate a good correlation between the estimation from MD simulation and calculation by Eqs. (17) and (25). The oscillations of Q_k [Eq. (25)] at $k > 5$ are caused by the transfer from exact Legendre functions to their approximation [Eq. (22)]; insignificant discrepancies at $k > \Lambda$ are of no interest because of a minor role of the capillary fluctuations in this region. Similar calculations were performed using the cluster configurations from the previous simulation for $g = 3000$ and $T = 0.75$ and 0.67. The same $\kappa = 0.548$ provides the best fit to Q_k in these cases as well, whence it follows that this value is independent of the cluster size (if the cluster is sufficiently large to isolate its surface particles) and can be applied to a flat liquid–vapor interface. Moreover, the constancy of κ is also indicative of a nontrivial fact that *the ratio γ/γ_0 is temperature independent*.

Based on the results of previous and recent MD simulations discussed above, the total variance of the cluster surface σ^2 defining the interface width was calculated (Fig. 4). This quantity can be evaluated by a direct calculation of the surface particles radial unweighted variance

$$\sigma^2 = \left\langle \frac{1}{g_s}\sum_{i=1}^{g_s} r_i^2 - \left(\frac{1}{g_s}\sum_{i=1}^{g_s} r_i\right)^2 \right\rangle, \qquad (30)$$

where g_s is the total number of cluster surface particles; averaging is performed over cluster configurations. The second estimation comes from the relation

$\sigma^2 = (1/2)\sum_{k=1}^{k_{\max}} S_k$. It can be seen that both estimates are close. The direct estimate is insignificantly higher than spectral one, probably, due to overestimated unweighted large deviations and somewhat depressed short-wavelength region of slice spectra.

The surface variance can be analytically estimated using Eqs. (6) and (19): $\sigma^2 = \sigma_b^2 + \sigma_c^2$. Figure 4 demonstrates a good agreement with the results arising from MD simulation both in the slope of a curve and its height. The slope is noticeably improved as compared to the early version of CWM,[12] where

$$\sigma^2 = \frac{T}{4\pi\gamma} \ln \frac{(2\Lambda_0 - 1)(2\Lambda_0 + 5)}{7}, \quad \Lambda_0 = 2.2g^{1/3}, \quad (31)$$

due to the difference between γ and γ_0 not taken into account in Eq. (31). The neglect of bulk fluctuations results in the underestimation of the line height (Fig. 4).

It was noted in the foregoing that Q_k is almost independent of simulation parameters, in particular, of the slice width, at least, in the region of capillary fluctuations $k < \Lambda$. However, the form of spectrum depends on the number of points of the analytical grid. If we adopt a certain definition of the surface particles, a problem of the fluctuation surface determination arises. It has been proposed in Ref.[5] to find a surface that includes the surface particles and has the minimum surface area. We have adopted other definition: the fluctuation surface has the same variance as the surface particles. This definition makes it possible to calculate straightforwardly one of the most important properties of the interface, its width. For the sake of simplicity, consider one-dimensional slice spectra. Since the coordinates $(r_i,\, \varphi_i)$ of surface particles form a random grid, the *weighted* variance is

$$\sigma^2 = \left\langle \frac{1}{2\pi} \sum_{i=1}^{g_{cs}} (\varphi_{i+1} - \varphi_i) r_i^2 - \left[\frac{1}{2\pi} \sum_{i=1}^{g_{cs}} (\varphi_{i+1} - \varphi_i) r_i \right]^2 \right\rangle, \quad (32)$$

which includes two integral sums, and the surface particles are numbered counterclockwise. If we pass on to the analytical grid, it is sufficient to select any constant difference between the points satisfying the condition $\Delta\varphi < \min\{\varphi_{i+1} - \varphi_i\}$ to rewrite Eq. (32) in the form

$$\sigma^2 \simeq \left\langle \frac{1}{2k_{\max}} \sum_{j=1}^{2k_{\max}} r_j^2 - \left[\frac{1}{2k_{\max}} \sum_{j=1}^{2k_{\max}} r_j \right]^2 \right\rangle, \quad (33)$$

where $2k_{\max} = 2\pi/\Delta\varphi$ is the number of analytical grid points and $r_j = r_i(\varphi_i)$; φ_i is the random grid point closest to the j th point on the analytical grid. However, if $\Delta\varphi$ is too small the unphysical tail area of the spectral density extends too much. An optimum value used in the previous and this study, which was found to agree on the average with above-mentioned condition, was found to be $k_{\max} = 0.9g_{cs}$. The procedure of the numerical Fourier analysis conserves the variance for each slice,

$$\frac{1}{2k_{\max}} \sum_{j=1}^{2k_{\max}} r_j^2 - \left[\frac{1}{2k_{\max}} \sum_{j=1}^{2k_{\max}} r_j \right]^2 = \frac{1}{2} \sum_{k=1}^{k_{\max}} \left[\left(\alpha_k^{(l,m)}\right)^2 + \left(\beta_k^{(l,m)}\right)^2 \right], \quad (34)$$

so that the spectral analysis performed in this paper ensures a correct width of the liquid–vapor interface.

V. CONCLUSIONS

In this paper, we have evaluated the contributions from capillary and bulk fluctuations to the total equilibrium fluctuations of cluster surface. Since we see no way to expand each individual configuration of the particles at the free cluster surface into the sum of certain bulk and capillary fluctuations, the configurations with zero capillary or bulk fluctuations were created artificially. The case of the bulk fluctuations was shown to be realized for clusters truncated by a spherical surface. The wave number spectrum of bulk fluctuations proved to be generated primarily by the discontinuity of cluster particles spatial distribution, which can be considered as a uniform random one. Since the spectrum of bulk fluctuations depends on the ratio of the wave number to the radius of a truncated cluster, it can be calculated for any cluster size by scaling. Subtraction of the bulk fluctuations spectrum from the total equilibrium spectrum of a free surface yields the net spectrum of capillary fluctuations. To evaluate the slice spectra obtained in MD simulation, we constructed the surface particles configurations in the form of individual spherical harmonics with zero bulk fluctuations. The slice spectra obtained for such configurations can be compared with the MD net capillary spectra.

The one-dimensional Fourier analysis of the slice spectra seems to be the only appropriate one, in contrast to a 2D analysis. In fact, the ratio of the average squared amplitude of a capillary fluctuation with $l = \Lambda$, $R^2 \left\langle |a_{\Lambda m}|^2 \right\rangle$, to the squared bulk liquid length scale r_ℓ^2 is $R^2 \left\langle |a_{\Lambda m}|^2 \right\rangle / r_\ell^2 \simeq T/\gamma_0 r_\ell^2 \Lambda^2$ [Eq. (11)]. For $T = 0.75$, $g = 30000$, $T/\gamma_0 r_\ell^2 \approx 3.91$, and $\Lambda = 29$, $R^2 \left\langle |a_{\Lambda m}|^2 \right\rangle / r_\ell^2 \approx 4.6 \times 10^{-3}$. Apparently, amplitudes of the shortest-wavelength capillary fluctuations are too small to perform a 2D spectral analysis numerically.

A comparison between the slice spectra of constructed capillary fluctuations and MD net spectra shows that it is sufficient to introduce the intrinsic surface tension γ_0, which is *independent on the wave number*, in contrast to the effective surface tension introduced for the total spectrum.[5] This property of γ_0 allows to deduce a balanced relation between the excess surface area induced

by the capillary fluctuations (rather than the bulk ones) and their equilibrium spectral amplitudes defined by the constant ratio γ/γ_0 [Eq. (16)]. Note that the excess surface area is also defined by the cutoff Λ, which is appreciably smaller than Λ_0 corresponding to the interparticle distance (for $g = 30000$, $\Lambda_0/\Lambda \approx 2.4$).

It was shown in this paper that the net capillary fluctuations spectrum obtained in MD simulation can be fitted by the theory with a single adjustable parameter $\kappa = 0.548$, which is independent of the cluster size and temperature. Therefore, it can be considered as a universal one and is suitable for a flat interface as well. Apparently, this universality can be accounted for by formation of virtual chains, which can be treated as the development of an instability of the fluctuation surface with a considerable curvature. Since κ is of the same order of magnitude as the maximum of $|\nabla\xi(\vartheta, \varphi)|$, we can suppose that virtual chains are formed at those surface points, where $|\nabla\xi(\vartheta, \varphi)| \gtrsim 1$. Hence, the curvature radius must be of the same order of magnitude as the interparticle distance, which is much smaller than the cluster radius if $g \gg 1$. This explicates why κ is independent of g. Formation of a virtual chain seems to be weakly dependent on the temperature. The reason for this may be expanded temperature region of a transition between the compact and virtual chain cluster structure.[15] It was noted in Ref.[16] that highly curved regions of the interface detach clusters thus limiting its curvature. In Ref.[16], MD simulation was performed at high temperatures not far from the critical point. Since our simulations correspond to temperatures closer to the melting point, we can assume that in our case the curvature is limited due to formation of the virtual chains, which are in turn the source of evaporating particles.

The definition of surface particles used in this study, which made it possible to treat the fluctuation surface, is most suitable at the temperatures not too far from the triple point. It is of special interest how close to the critical point this definition can be applied. As the temperature is increased from the triple point to critical one, the ratio of liquid and vapor densities decreases, and the average interface width becomes large compared to the molecular diameter. At sufficiently high temperatures, the concentration of small clusters in the vapor phase may be comparable to that of monomers. One can speculate that such clusters may be attached to the liquid–vapor interface rather than virtual chains, which may require a sophisticated definition of the surface particles including the procedure of overhangs elimination. The situation may be complicated by the fact that the contribution from overhangs to the average system density distribution is no longer negligibly small. Strong nonideality of the vapor may force a reconsideration of the liquid phase identification as well. On the other hand, it follows from Ref.[16] that the instantaneous interface density profile is abrupt even at the temperatures compared to the critical one, albeit the surface form fluctuations are great. Since our definition is based on this interface property, one can assume that it may be valid for the most part of the interval between triple and critical temperatures. An investigation of the surface fluctuations at high temperatures including the mechanism of overhangs formation will be addressed in the future work.

* Electronic address: dmrzhu@yandex.ru

1. J. Rowlinson and B. Widom, Molecular Theory of Capillarity (Clarendon, Oxford, 1982).
2. F. P. Buff, R. A. Lovett, and F. H. Stillinger, Phys. Rev. Lett. **15**, 621 (1965).
3. T. Hiester, S. Dietrich, and K. Mecke, J. Chem. Phys. **125**, 184701 (2006).
4. P. Tarazona, R. Checa and E. Chacón, Phys. Rev. Lett. **99**, 196101 (2007).
5. P. Tarazona and E. Chacón, Phys. Rev. B **70**, 235407 (2004).
6. J. Chowdhary and B. M. Ladanyi, J. Phys. Chem. B **110**, 15442 (2006).
7. J. Chowdhary and B. M. Ladanyi, Phys. Rev. E **77**, 031609 (2008).
8. E. Chacón, P. Tarazona, and J. Alejandre, J. Chem. Phys. **125**, 014709 (2006).
9. F. H. Stillinger, J. Chem. Phys. **128**, 204705 (2008).
10. D. I. Zhukhovitskii, J. Chem. Phys. **125**, 234701 (2006).
11. D. I. Zhukhovitskii, J. Exp. Theor. Phys. **94**, 336 (2002).
12. N. Pavloff and C. Schmit, Phys. Rev. B **58**, 4942 (1998).
13. F. H. Stillinger, J. Chem. Phys. **76**, 1087 (1982).
14. L. Rayleigh, Proc. R. Soc. London **29**, 71 (1879).
15. D. I. Zhukhovitskii, J. Chem. Phys. **110**, 7770 (1999).
16. S. I. Anisimov and V. V. Zhakhovskii, Pis'ma Zh. Eksp. Teor. Fiz. **57**, 91 (1993); V. V. Zhakhovskii and S. I. Anisimov, JETP **84**, 734 (1997).